Earprint: Transient Evoked Otoacoustic Emission for Biometrics

Yuxi Liu and Dimitrios Hatzinakos, *Senior Member, IEEE*

***Abstract*— Biometrics is attracting increasing attention in privacy and security concerned issues, such as access control and remote financial transaction. However, advanced forgery and spoofing techniques are threatening the reliability of conventional biometric modalities. This has been motivating our investigation of a novel yet promising modality transient evoked otoacoustic emission (TEOAE), which is an acoustic response generated from cochlea after a click stimulus. Unlike conventional modalities that are easily accessible or captured, TEOAE is naturally immune to replay and falsification attacks as a physiological outcome from human auditory system. In this paper, we resort to wavelet analysis to derive the time-frequency representation of such nonstationary signal, which reveals individual uniqueness and long-term reproducibility. A machine learning technique linear discriminant analysis is subsequently utilized to reduce intrasubject variability and further capture intersubject differentiation features. Considering practical application, we also introduce a complete framework of the biometric system in both verification and identification modes. Comparative experiments on a TEOAE data set of biometric setting show the merits of the proposed method. Performance is further improved with fusion of information from both ears.**

***Index Terms*— Robust biometric modality, transient evoked otoacoustic emission, time-frequency analysis, linear discriminant analysis, biometric fusion.**

I. Introduction

BIOMETRICS systems are rapidly supplanting traditional identity management systems (e.g., passwords, access card), by utilizing the uniqueness of physiological, biological or behavioral traits of an individual. For example, e-passport embeds one's face and/or iris characteristics to verify the identity; fingerprint recognition is widely used in access control, laptop lock and mobile device security.

Along with the pervasion of biometrics technologies, however, sophisticated forgery and spoofing techniques are threatening the reliability of conventional biometric modalities. For instance, fingerprints can be easily captured from a glass surface, phone screen or anywhere one touched, and an artificial clone can be created by cheap and readily available plastic mold and gelatin [1]. Moreover, signature and voice recognition system become vulnerable against sophisticated falsification attacks. Such vulnerability has been motivating the recent investigation of a novel yet promising biometric modality Transient Evoked Otoacoustic Emission (TEOAE) [2]–[4], which is naturally immune to replay and falsification attacks as a physiological signal from human auditory system.

TEOAE refers to an approximate 20 ms acoustic response generated by an active process occurring inside the cochlea after a low level transient click stimulus [5]. TEOAE is present in most normal ears (99+%) [6] and widely used in clinical applications as a diagnostic tool for hearing assessment [7]. Importantly, a number of biological and clinical studies [6], [8], [9] have reported that TEOAE recordings show significant differences among individuals, due to different inner ear structure and many other genetic factors. Such uniqueness enables its role in identity recognition as "fingerprints" or "signature".

The remainder of this paper is structured as follows: Section II first provides an overview of ear structure and generation of TEOAE, as well as feasibilities and perks of using TEOAE for biometrics. Section III is a review of related works and elaboration on the existing issues to be addressed. Section IV presents detailed methodology of biometrics based on TEOAE along with a complete system framework. They are followed by Section V where experimental results and analysis are presented. Lastly, our work is concluded in Section VI.

II. Transient Evoked Otoacoustic Emission

A. Overview of Otoacoustic Emission

The human ear, which mainly consists of outer ear, middle ear and cochlea (inner ear), is a fully developed part of our bodies at birth. Sound collected by outer ear travels along the ear canal and middle ear and arrives at the cochlea. Inside the cochlea, basilar membrane responds to different frequency in a location-specific way, where higher frequencies are responded near the base and lower frequencies near the apex. Resting on the basilar membrane, there are two types of cells of particular importance to auditory system, the outer hair cells (OHCs) acting as low-level sound amplifiers, and inner hair cells responsible for transformation of the sound vibrations into electrical signals that are then relayed to the auditory cortex.

In mammals, in order to enhance cochlear sensitivity and frequency selectivity (i.e., discrimination of hearing), OHCs vibrate and act as energy sources for the forward amplification of sound. The active movement of OHCs, meanwhile, generates a nearly inaudible sound, i.e., otoacoustic

Manuscript received April 18, 2014; revised July 15, 2014 and August 11, 2014; accepted September 17, 2014. Date of publication October 1, 2014; date of current version November 12, 2014. This work was supported in part by the Natural Sciences and Engineering Research Council of Canada and in part by the Ontario Brain Institute, Toronto, ON, Canada. The associate editor coordinating the review of this manuscript and approving it for publication was Prof. Sviatoslav S. Voloshynovskiy.

The authors are with the Edward S. Rogers Sr. Department of Electrical and Computer Engineering, University of Toronto, Toronto, ON M5S 3G4, Canada (e-mail: yxliu@ece.utoronto.ca; dimitris@comm.utoronto.ca).

Color versions of one or more of the figures in this paper are available online at http://ieeexplore.ieee.org.

Digital Object Identifier 10.1109/TIFS.2014.2361205

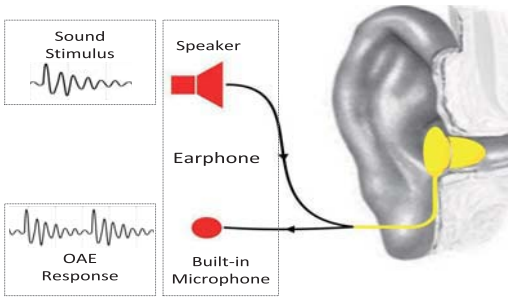

Fig. 1. Using earphone with built-in microphone for OAE measurement.

emission (OAE). The resulting OAE then echoes back to ear canal through middle ear and thus can be easily measured with an earphone with a built-in microphone or a small probe inserted into the ear canal (Figure 1). A more thorough review of the ear structure and generation of OAE can be found in [6].

B. Types of Otoacoustic Emission

There are, in fact, different types of OAE that are determined by the sound stimulus used to generate the response. They are summarized into three categories:

1) Spontaneous Otoacoustic Emission (SOAE): Low-level sound continuously emitted without any presentation of an acoustic stimulus. SOAEs occur in only about 60% of ears with normal hearing [6], and thus it is not prevalent in clinical use.

2) Distortion Product Otoacoustic Emission (DPOAE): Evoked OAE as a result of intermodulation distortion in response to two simultaneously presented pure-tone stimuli of different frequencies [7]. The prevalence of DPOAE reaches 99+% of normal hearing ears, which is as same as that of TEOAE. However, DPOAE measurement system has high hardware requirements, including a probe with two speakers generating stimulus of different frequencies and a microphone associated with an analog-to-digital converter (ADC) to distinguish the response from the sinusoidal waveform stimuli.

3) Transient Evoked Otoacoustic Emission (TEOAE): Acoustic response stimulated by a short low level click sound, which is a flat-band signal in frequency domain. TEOAE emerges shortly after the click stimulus diminishes and lasts approximately 20 ms. An example of the stimulus and TEOAE recording from the dataset collected in Biometrics Security Laboratory at the University of Toronto [10] is displayed in Figure 2 (Section V-A describes the dataset in detail).

In human cochlea, a tone-burst stimulus can excite the basilar membrane and evoke a frequency-specific response; when a broadband click stimulus is used, the evoked emission becomes a cumulative response consisting of several dominant frequency components with different latency [11]. This makes TEOAE highly non-stationary with a complex waveform compare to other OAE signals.

As aforementioned, TEOAE, as a simple and non-invasive tool for hearing assessment, is prevalently used in universal infant hearing screening programs; placing the probe for TEOAE measurement is similar to wearing an earphone; interpersonal differences of TEOAE signal suggest an individual

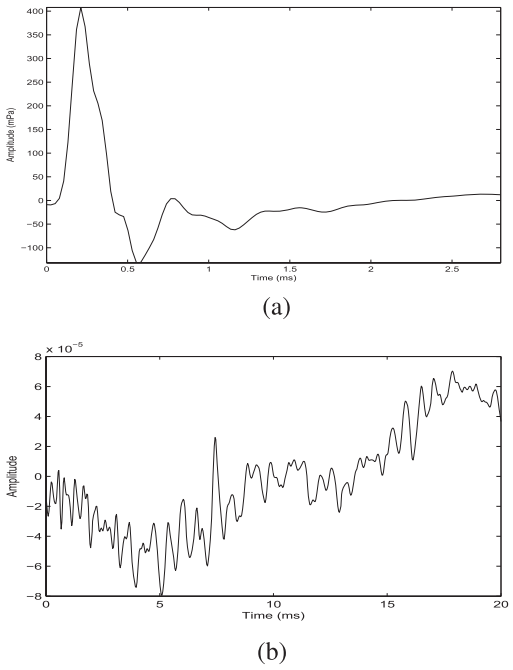

Fig. 2. Example of (a) the click stimulus, (b) a corresponding TEOAE recording.

morphology of inner ears especially OHCs. Together with its collectability, universality and uniqueness, the stability proved by the high reproducibility both on short-term and on long-term progression, which is discovered in clinical tests and biological studies [12], [13], essentially makes it a feasible biometric modality.

Using TEOAE for biometrics has several advantages. Primarily, the inherent robustness against falsification and replay attacks: fabricating one's auditory system is almost impossible; also it is extremely difficult to steal one's TEOAE which is the outcome of physiological activities of the auditory perception in response to a specific acoustic stimulation. This likewise enhances biometric reliability and effectiveness with implicit liveness detection. Further, it can be employed to some special scenarios where face and fingerprint recognition fail to work, such as neonate identification. Last but not least, framework of TEOAE biometrics can be readily integrated into multimedia devices with headset or earphone (e.g. smart phone, media player) for user authentication and personal data security.

III. Related Works

In 2004, a primary study of TEOAE for biometrics was introduced by Swabey et al. [14] by analyzing the Euclidean distance of the frequency components in the power spectra of the signal. After that, a quantitative study was conducted in [15] to approximate the probability density function (PDF) of the intra- and inter-class distance distributions by maximum likelihood estimation (MLE) to the time series data. In [16], cepstrum transformation was applied for feature extraction and pairwise distance was calculated in both temporal and cepstral domain. This has provided a potential route to better extract TEOAE biometric features by applying time-frequency analysis.

Recently, Grabham et al. [3] summarized the above works [14], [15], examined biometric verification performance in 4 datasets of TEOAE recorded in the same session respectively (either in one sitting or with the ear probe removed and refitted shortly), which was of little biometric value without considering the high intra-subject variability in separate recording sessions. The reported equal error rate (EER) of the first 3 datasets was 2.30% (measured), 2.29% (predicted) and 4.58% (predicted) respectively.

TEOAE Dataset in biometric setting was first investigated in [2], where Bivariate Empirical Mode Decomposition (BEMD) was applied to decompose a signal into multi-level local oscillation components with selected frequencies. Correlations across different levels were then calculated to derive the matching scores. Empirical weights for score computation were chosen based on limited testing data (only one TEOAE from 54 subjects) without statistical analysis, which failed to guarantee generalizability and applicability among large population.

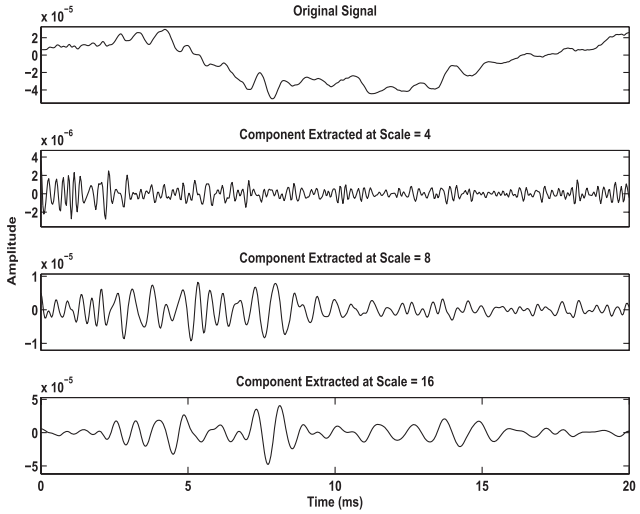

Fig. 3. Three different frequency components extracted from original signal at scale $= 4, 8, 16$ respectively.

IV. The Proposed Approach to TEOAE Based Biometrics

In this work, we derive the time-frequency representation of the original signal by adopting wavelet analysis to reveals individual uniqueness and long-term reproducibility. Considering the time-variant nature of such physiological signal, we apply discriminant analysis to further reduce the intra-subject variability prior to matching procedure. Lastly, we introduce a complete framework of the biometric system in both verification and identification modes. Specifically, similarity score is measured in Pearson correlation in the first mode; best matching identity is attained by multiclass classifier softmax regression in the latter one.

A. Time-Frequency Representation

TEOAE is a cumulative response due to the fact that the broadband stimuli can excite the entire basilar membrane and different resulting frequency components arrive at the ear canal at different times. Hence, investigating TEOAE signal in either time domain or frequency domain is suboptimal. Analysis through a time-frequency approach is therefore advisable based on its close relation with cochlear mechanisms [17].

In this work, continuous wavelet transform (CWT) [18] is applied to separate the mixed frequency components and derive the time-frequency representation of TEOAE. Regarding mother wavelet $\psi(t)$, which is a narrow band-pass function, the wavelet transform to a signal $x(t)$ is given by:

$$WT_x(a,b) = \frac{1}{\sqrt{a}} \int_{-\infty}^{+\infty} x(t)\psi^*(\frac{t-b}{a})dt \qquad (1)$$

where $\psi(\frac{t-b}{a})$ is the corresponding window function with scale factor a and time translation factor b. Let $X(\omega)$ and $\Psi(\omega)$ be the Fourier transform of $x(t)$ and $\psi(t)$ respectively. The equivalent frequency-domain version of wavelet transform is:

$$WT_x(a,b) = \frac{1}{2\pi} \int_{-\infty}^{+\infty} X(\omega)\Psi^*(a\omega)e^{+j\omega b}d\omega \qquad (2)$$

The adjustable window function is introduced so that the mixed frequency components in TEOAE can be separated. More precisely, if the narrow band-pass mother wavelet $\Psi(\omega)$ is centered around frequency f_0, according to Fourier transform theorems, $\Psi(a\omega)$ is the same function centered at $f_c = f_0/a$ with constant quality factor. Different frequency components can be therefore extracted from the original signal by different scales. As Figure 3 displays, three frequency components are extracted from the original TEOAE signal at scale $= 4, 8, 16$ respectively with Daubechies 5 as mother wavelet. A higher frequency fraction corresponds to a smaller scale and vice versa.

Further, variation of scale alters not only the central frequency f_c of the band-pass function, but also the window length in time. Specifically, the time-duration is inversely proportional to f_c. By virtue of this particular structure of the wavelet filters, wavelet transform can provide highly accurate extraction of the time-frequency features from a mixed signal with high frequency components of brief duration and low frequency ones of long duration, TEOAE is such a case [17], [19]. As depicted in Figure 3, the discriminated frequency components show a clear difference in time duration, i.e., a longer latency for a lower frequency component (higher scale). CWT preserves good resolution in both time and frequency domain and thus is a suited approach for feature extraction of TEOAE.

A particular frequency component extracted is then used to represent the original signal if it can well differentiate ("identify") itself from those of other sources. Take two subjects in the dataset [10] for example, frequency components at scale $= 8$ are extracted from both subjects per different recording session respectively. Extracted components from the same subject (A or B) exhibit high similarity between different sessions (Figure 4 (a) and (b)) although their original signals look disparate. However, extracted components from different subjects (A and B) highly diverge despite the close waveform of their original signals (Figure 4 (c)). Time-frequency representation reveals the intra-subject stability or

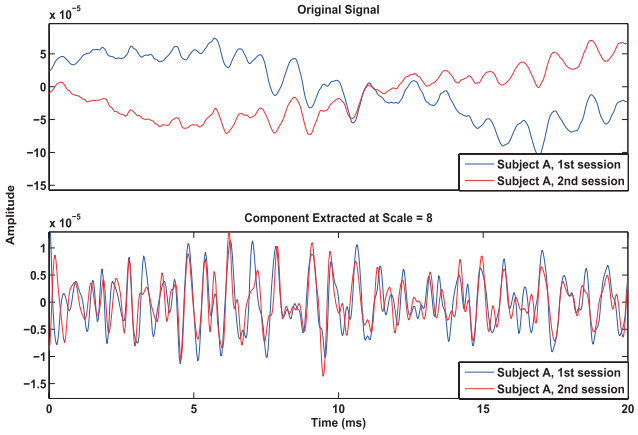

(a)

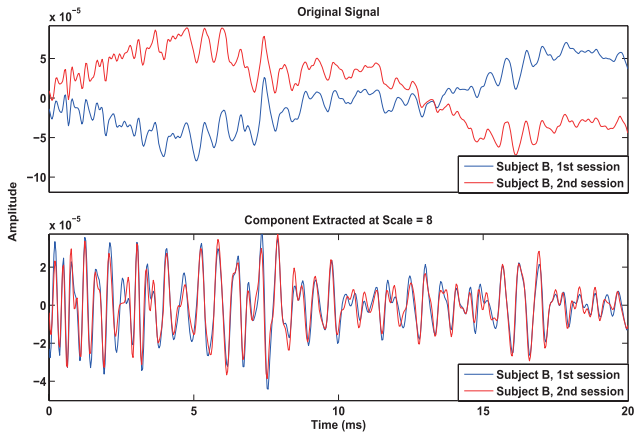

(b)

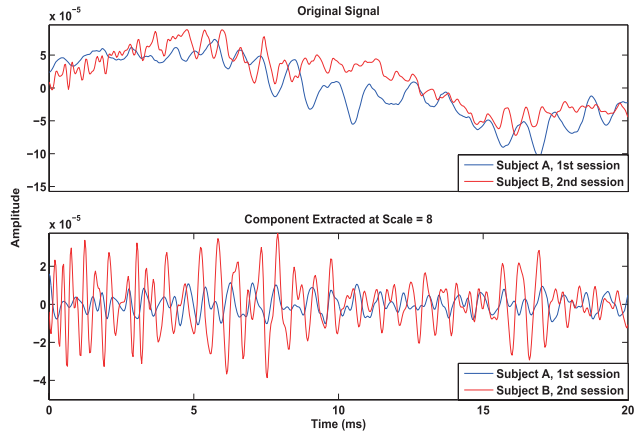

(c)

Fig. 4. Frequency components extracted from signal of (a) subject A in the 1st and the 2nd session, (b) subject B in the 1st and the 2nd session, (c) subject A in the 1st and subject B in the 2nd session.

reproducibility and the inter-subject disparity that are obscure in original signals.

B. LDA-Based Dimensionality Reduction

The resulting TEOAE time-frequency representation vectors can be directly used for matching. However, unlike most conventional biometric modalities, e.g., fingerprints and iris, TEOAE as a physiological signal is time-variant over a long time period with observed changes in the waveform morphology, and so is the corresponding time-frequency feature derived from it (see Figure 4 (a) for example). Due to this dynamic nature, it is important to further diminish the intra-subject variability in order to reduce false rejection. Besides, the dimensionality of the time-frequency representation vector is as same as that of the original signal (see Figure 4). Dimensionality reduction is therefore prudent to avoid possible redundance and irrelevance of the features, and additionally to save storage space for template data in a biometric system. For these reasons, a supervised subspace learning method linear discriminant analysis (LDA) [20], [21] is performed in this work to select more effective features in a class-optimal way prior to matching procedure.

The objective of LDA is to preserve the maximum amount of class separability information with the minimum-dimensional data after linear projection. Details of the implementation are herein discussed, beginning with the following definitions:

- Suppose we have a training set consisting of K classes, i.e., K subjects registered in the biometric system.
- Let N_k be the number of time-frequency representation vectors from class k, where $k = 1 \ldots K$.
- $\mathbf{z}_{ki}$ is defined as a representation vector (observation, sample) from class k, where $i = 1 \ldots N_k$.
- The training feature set comprises $\mathbf{Z}_1, \mathbf{Z}_2, \ldots, \mathbf{Z}_K$, where $\mathbf{Z}_k = \{\mathbf{z}_{k1}, \mathbf{z}_{k2}, \ldots . \mathbf{z}_{kN_k}\}$ is the group of observations from class k.
- Let $\boldsymbol{\mu}_k$ be the class mean vector for class k, i.e., $\boldsymbol{\mu}_k = \frac{1}{N_k} \sum_{i=1}^{N_k} \mathbf{z}_{ki}$.
- Further, $\boldsymbol{\mu}$ is the overall mean vector.

The feature extraction procedure of LDA is a linear transformation which maps the high-dimensional data onto a m-dimensional ($m = K - 1$) space where between-class distance is maximized and within-class distance is minimized, so that observations are best separated into classes. Two types of distance are respectively measured in between-class and within-class scatter matrices $\mathbf{S}_b$ and $\mathbf{S}_w$, which are computed as below:

$$\mathbf{S}_b = \sum_{k=1}^{K} N_k (\boldsymbol{\mu}_k - \boldsymbol{\mu})(\boldsymbol{\mu}_k - \boldsymbol{\mu})^T \tag{3}$$

$$\mathbf{S}_w = \sum_{k=1}^{K} \sum_{i=1}^{N_k} (\mathbf{z}_{ki} - \boldsymbol{\mu}_k)(\mathbf{z}_{ki} - \boldsymbol{\mu}_k)^T \tag{4}$$

Accordingly, the projection weight $\mathbf{W}$ should maximize the Fisher criterion function $J(\mathbf{W})$:

$$\mathbf{W} = \arg\max_{\mathbf{W}} J(\mathbf{W}) = \arg\max_{\mathbf{W}} \frac{|\mathbf{W}^T \mathbf{S}_b \mathbf{W}|}{|\mathbf{W}^T \mathbf{S}_w \mathbf{W}|} \tag{5}$$

which guarantees largest segregation between observations from different classes and smallest variance within those from the same classes.

The optimum $\mathbf{W}^*$ can be obtained by computing the m most significant eigenvectors which correspond to the

m largest eigenvalues of $\mathbf{S}_w^{-1}\mathbf{S}_b$. The projected feature vector $\tilde{\mathbf{z}}_{ki}$ ($\tilde{\mathbf{z}}_{ki} \in \Re^m$) for a training sample $\mathbf{z}_{ki}$ is consequently expressed as:

$$\tilde{\mathbf{z}}_{ki} = \mathbf{W}^{*T}\mathbf{z}_{ki} \tag{6}$$

and is stored in the system gallery as a reference template. $\mathbf{W}^*$ is also saved in the system and will be reapplied to a new input feature vector $\mathbf{z}'$ so that it is projected onto the optimal and comparable subspace, i.e., $\tilde{\mathbf{z}}' = \mathbf{W}^{*T}\mathbf{z}'$.

C. Biometric Matching

After LDA-based feature extraction from time-frequency representations, the next procedure is biometric matching which compares the probe against the templates stored in system gallery. Depending on a specific application, there are two modes of matching to contemplate, verification and identification. The matching module of a biometric system either validates a user's claimed identity or establishes an unknown user's identity.

1) Verification: Verification is basically a one-to-one matching, comparing the input sample presented by a user against the template corresponding to the claimed identity which is stored in the system. The decision of match or non-match is finally made based on the similarity score and a pre-defined threshold. Briefly, biometric verification aims to answer the question "*Is this user the one he/she claims to be?*".

In this work, Pearson's distance is chosen as a metric, which is defined from the Pearson correlation coefficient as a common similarity measure in biometrics. Depending on application scenario, biometric verification can be categorized into two sets, closed and open:

In closed-set verification, one of the pre-enrolled individuals is to be authenticated as what he/she claims. For instance, to request access to a facility of a company, an employee contributes personal biometric sample and makes an identity claim by presenting employee ID card or badge. Since all users (genuine and illegitimate) are known to the system beforehand, the class-optimal feature sets after LDA can be used for matching, which will largely improve system performance. The similarity score S_P between a probe vector $\tilde{\mathbf{z}}'$ and the reference template $\tilde{\mathbf{z}}_k$ from the claimed identity k is calculated by:

$$S_P(\tilde{\mathbf{z}}', \tilde{\mathbf{z}}_k) = 1 - \frac{cov(\tilde{\mathbf{z}}', \tilde{\mathbf{z}}_k)}{\sqrt{cov(\tilde{\mathbf{z}}', \tilde{\mathbf{z}}')cov(\tilde{\mathbf{z}}_k, \tilde{\mathbf{z}}_k)}} \tag{7}$$

where $cov(\mathbf{a}, \mathbf{b})$ is the covariance matrix of $\mathbf{a}, \mathbf{b}$. An ACCEPT decision is made only if $S_P(\tilde{\mathbf{z}}', \tilde{\mathbf{z}}_k) \leq t_P$, where t_P is the corresponding decision threshold.

In open-ended scenario, attacks in most cases are from imposters unregistered or unknown to the system in advance. For instance, a thief attempts to be authenticated on a smart phone. In this case, the probe and template can only be compared in the original representation space (without LDA) rather than class-optimal subspace, where information of all classes should be considered and no new class is allowed. The similarity score S_P between a probe vector and the reference template is calculated on respective representation vectors after CWT $\mathbf{z}'$ and $\mathbf{z}_k$:

$$S_P(\mathbf{z}', \mathbf{z}_k) = 1 - \frac{cov(\mathbf{z}', \mathbf{z}_k)}{\sqrt{cov(\mathbf{z}', \mathbf{z}')cov(\mathbf{z}_k, \mathbf{z}_k)}} \tag{8}$$

2) Identification: In identification mode, the system checks the probe presented by an unknown individual against the templates in the dataset from all enrollees in attempt to establish his/her identity. Biometric identification is basically a one-to-many comparison process, which is equivalent to multiclass classification. It seeks to answer the question "*What is the identity of this person?*".

An efficient and accurate multiclass classifier softmax regression, also known as multinomial logistic regression [22], [23], is employed in this work. It generalizes binary logistic regression by allowing the model to learn and predict more than two categorical values. Similarly, it uses maximum likelihood estimation (MLE) to evaluates the probabilities of different possible outcomes.

Given a training set $\{(\mathbf{z}^{(1)}, y^{(1)}), (\mathbf{z}^{(2)}, y^{(2)}), \ldots, (\mathbf{z}^{(M)}, y^{(M)})\}$, where $\mathbf{z}^{(i)}$ is an input feature vector consisting of the optimal feature vector after dimensionality reduction and an appended dimension for the intercept term, i.e., $\mathbf{z}^{(i)} \in \Re^{m+1}$ (here for convenience, we also write $\mathbf{z}$ to denote the optimal features after LDA, instead of $\tilde{\mathbf{z}}$); $y^{(i)} \in \{1, 2, \ldots, K\}$ is the corresponding class label; and M is the number of training samples. Let $\boldsymbol{\theta} = \{\boldsymbol{\theta}_1, \boldsymbol{\theta}_2, \ldots, \boldsymbol{\theta}_K\}$ denote the parameters of the regression model to be estimated, where $\boldsymbol{\theta}_k \in \Re^{m+1}$ represents the coefficients of class k for each input feature vector. The hypothesis that $\mathbf{z}^{(i)}$ is classified as class j is written as:

$$P(y^{(i)} = j|\mathbf{z}^{(i)}, \boldsymbol{\theta}) = \frac{\exp(\boldsymbol{\theta}_j^T\mathbf{z}^{(i)})}{\sum_{k=1}^K \exp(\boldsymbol{\theta}_k^T\mathbf{z}^{(i)})} \tag{9}$$

Also note that $1/\sum_{k=1}^K \exp(\boldsymbol{\theta}_k^T\mathbf{z}_i)$ is the normalization factor so that

$$\sum_{j=1}^K P(y^{(i)} = j|\mathbf{z}^{(i)}, \boldsymbol{\theta}) = 1 \tag{10}$$

for any i.

Model parameters are then learned from the training data by MLE. The log-likelihood function to be maximized is defined as:

$$\begin{aligned} l(\boldsymbol{\theta}) &= \sum_{i=1}^M \log P(y^{(i)}|\mathbf{z}^{(i)}, \boldsymbol{\theta}) \\ &= \sum_{i=1}^M \left[\sum_{j=1}^K \mathrm{I}\{y^{(i)} = j\}\boldsymbol{\theta}_j^T\mathbf{z}^{(i)} - \log \sum_{k=1}^K \exp(\boldsymbol{\theta}_k^T\mathbf{z}^{(i)}) \right] \end{aligned} \tag{11}$$

where $\mathrm{I}\{*\}$ is the indicator function, i.e., $\mathrm{I}\{y^{(i)} = j\} = 1$ only if $\mathbf{z}^{(i)}$ indeed belongs to class j. The estimate $\boldsymbol{\theta}$ is given by:

$$\widehat{\boldsymbol{\theta}} = \arg\max_{\boldsymbol{\theta}} (l(\boldsymbol{\theta}) + \log p(\boldsymbol{\theta})) \tag{12}$$

with $p(\boldsymbol{\theta})$ being the prior of $\boldsymbol{\theta}$ in order to avoid overfitting,

$$p(\boldsymbol{\theta}) \propto \exp(-\lambda\|\boldsymbol{\theta}\|_2^2) = \exp(-\lambda \sum_{k=1}^K \|\boldsymbol{\theta}_k\|_2^2) \tag{13}$$

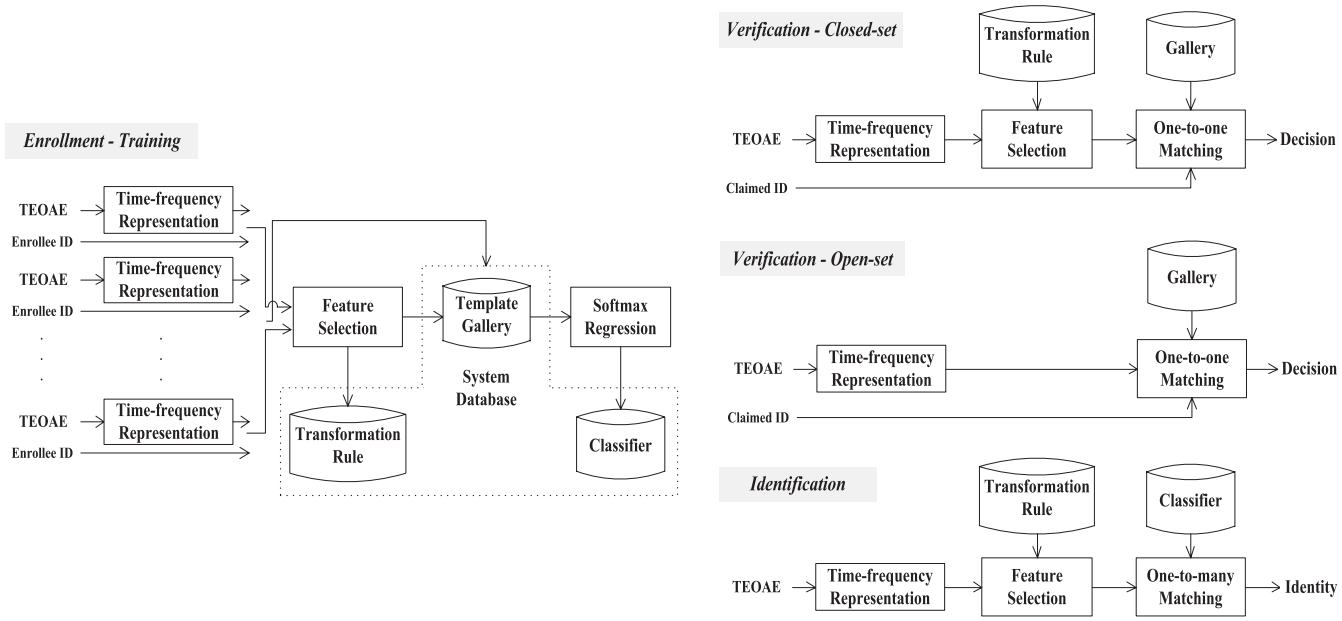

Fig. 5. Framework of the proposed biometric system.

where $\|\cdot\|_2$ denotes l_2 norm and λ ($\lambda \geq 0$) a regularization factor. Therefore, the prior acts as a regularizer on $\boldsymbol{\theta}$ and MLE in this way can be viewed as a penalized version or maximum a posteriori (MAP) estimation. The estimate in (12) is typically accomplished by an iterative optimization method such as gradient descent or Newton's method (e.g., L-BFGS [24] as the one we employ).

The well-trained model can be used to classify an unlabeled input $\mathbf{z}'$. The hypothesis function $h_{\boldsymbol{\theta}}(\mathbf{z}')$ will return a K-dimension vector with the estimated probabilities of each class:

$$h_{\widehat{\boldsymbol{\theta}}}(\mathbf{z}') = \begin{bmatrix} P(y'=1|\mathbf{z}', \widehat{\boldsymbol{\theta}}) \\ P(y'=2|\mathbf{z}', \widehat{\boldsymbol{\theta}}) \\ \cdot \\ \cdot \\ P(y'=K|\mathbf{z}', \widehat{\boldsymbol{\theta}}) \end{bmatrix} = \frac{1}{\sum_{k=1}^{K} \exp(\hat{\boldsymbol{\theta}}_k^T \mathbf{z}')} \begin{bmatrix} \exp(\hat{\boldsymbol{\theta}}_1^T \mathbf{z}') \\ \exp(\hat{\boldsymbol{\theta}}_2^T \mathbf{z}') \\ \cdot \\ \cdot \\ \exp(\hat{\boldsymbol{\theta}}_K^T \mathbf{z}')) \end{bmatrix} \tag{14}$$

The largest element indicates the most likely class that the input vector is labeled.

D. Framework of TEOAE Biometric System

Following all aforementioned modules, a complete framework of biometric system is logically proposed in this section. A general setup for the biometric system involves an enrollment stage and a verification and/or identification stage. A block diagram of the proposed system is depicted in Figure 5 and detailed explanation is provided as follows.

During the enrollment session, TEOAE is acquired from each enrollee and subjected to CWT-based time-frequency analysis at a particular scale. Resulting representation vectors are stored in template gallery and then used to drive the LDA-based optimal subspace learning algorithm. The fully trained transformation rule with weight $\mathbf{W}^*$, and resulting feature sets are stored in the system database (see the dash line in Figure 5). Notably for identification system, feature templates are further utilized to force the learning of softmax regression model. Optimized classifier with parameter $\widehat{\boldsymbol{\theta}}$ is included in the system database used for future prediction. In a word, the enrollment operation establishes the template pool and creates a paradigm of individual TEOAE morphologies, acting as a training procedure from machine learning perspective.

In the verification mode, an individual contributes a TEOAE recording and claims an identity k. For a closed-set scenario, probe feature vector will be generated after CWT and linear transformation according to the pre-trained rule. It is then matched against the respective class-optimal template of subject k retrieved from the gallery. For an open-set scenario, probe feature vector comes after CWT and is later compared with the respective representation vector template. And decision of either accept or reject the claim is finally made.

As for the identification operation, an individual from the pre-enrolled subject pool gets recorded. The biometric system will similarly conduct feature extraction and selection to a new reading, and compute the hypothesis function using the pre-determined classifier with the probe vector as an input. The user's identity will be consequently established after a one-to-many search.

E. Application Scenario

Nowadays, mobile devices have outgrown their initial use for communication and have added many powerful functionalities, such as data storage, web access and remote commerce, etc. The increasing need for greater mobile security has been opening up new areas in biometrics. Hence, the

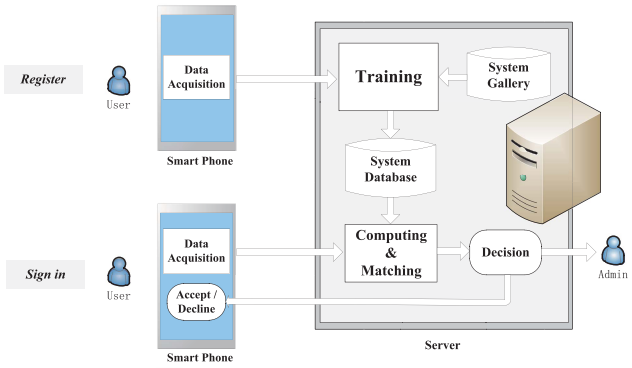

Fig. 6. Architecture of the TEOAE biometric system for identity authentication in mobile commerce.

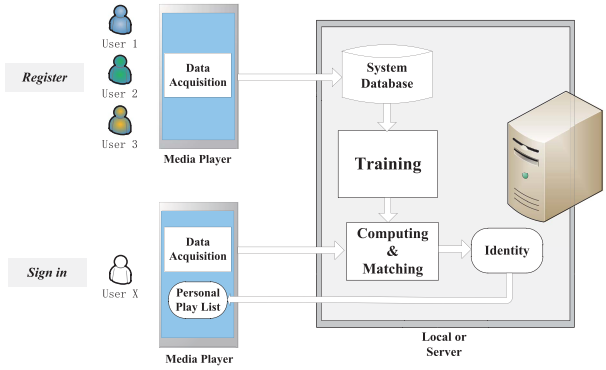

Fig. 7. Architecture of the TEOAE biometric system for personalization in multimedia device.

need for greater security for mobile devices and more robust protection against unauthorized use has been rapidly increasing.

As aforementioned, TEOAE is naturally immune to falsification or replay attacks as an outcome of physiological activity of the auditory perception. Besides, its compatibility with mobile devices and robustness make it an advantageous modality for mobile security. As an example, Figure 6 exhibits how the proposed system is applied to mobile commerce (e.g., remote banking, phone purchase). To fulfill registration for the secure system, a client's phone is responsible for TEOAE data acquisition and transmission to the remote server in the administrator's side, where data processing and learning algorithms are afterwards implemented. When a user (who is either the authorized client or an illegitimate one) is signing in, the server receives data sent from user's phone and performs matching after computation. It finally responds to both the administrator and the user whether the authentication is accepted or declined, whether follow-up transaction is allowed or refused. It is expected that security questions whose answers can be easily discovered (e.g., "What is your mother's maiden name?", "What is your date of birth?", "where did you go to college?") will no longer be asked.

Further, local application (e.g., user verification and identification, private data access) of the proposed biometric system share the same architecture, except that datasets are stored and computation is conducted locally or on a client-server with which the device needs to communicate. For instance, a multimedia device (e.g., ipod, MP4) can be used by multiusers. Each user has his/her own profile, including history, subscription channel and favourite play list. Utilizing TEOAE biometrics, automatic personalization can be realized. A user registers with the system when wearing the earphone at the first time. In later use, the user will be recognized by the system and automatically presented his/her preferred list without manually selecting. The conceptual framework is displayed in Figure 7.

V. Experiments and Results

A. Dataset and Experimental Setting

In our experiments, we make use of the biometric setting dataset with 54 subjects collected at the Biometrics Security Laboratory [10], at the University of Toronto (protocol reference #23018). Vivosonic Integrity System was used for data collection with recording protocol [2] listed in Table I. To alleviate constraints on the environment, the collection was conducted in a regular office with people conversing and ambulating, instead of a sound proof clinical setting.

TABLE I
TEOAE Recording Protocol

Stimulus Parameters	STI-Mode	Nonlinear
	Click Interval	21.12ms
	Click Duration	$80\mu s$
	Sound Level	80dB peSPL
Test Control	Record Window	$2.8-20$ms
	Low Pass Cut-off	6000 Hz
	High Pass Cut-off	750Hz
	Artifact Rejection Threshold	55dB SPL

For each subject, TEOAE signals were collected from the left and right ear respectively in each of two sessions. Time interval between different sessions was at least one week so as to verify the long-term stability for biometric evaluation purpose, which previous datasets in [3] nonetheless fail to achieve with ear probe removed and reinserted in single sitting (see Table II for the comparison of various datasets).

In each collection, number of recordings or length of collection time depends on how fast the response steadies, which varies by person, body condition and body movement, etc. Collection is stopped when the whole wave reproducibility (WWR) measure displayed on the Integrity system is high enough ($\geq$90%), which indicates high steadiness of response. Current dataset consists of in average 122 TEOAE recordings of length 17.2 ms for the left ear and 113 recordings for the right ear per person per session. Last 10 recordings of the first and second session per ear per subject, which are in general the 10 steadiest ones, are used to constitute the experimental training and testing set respectively. Daubechies 5 is again chosen as the mother wavelet of CWT.

Comparative experiments are first conducted in single ear scenario, using signals collected from either left or right ear. Results show the merit of the proposed method by comparing

TABLE II
COMPARISON OF VARIOUS DATASET PROPERTIES

Parameter	Dataset 1 in [3]	Dataset 2 in [3]	Dataset 3 in [3]	Dataset 4 in [3]	Our dataset [10]
No. of Subjects	23	760	561	33	54
No. of sessions per subject	10	2	2	4L + 4R	2L + 2R
Interval between sessions	Single sitting	Single sitting	Single sitting	Single sitting	**At least one week**
Environment	quiet room	clinic	clinic	regular office	regular office
Age Range of subjects	Adults 20-60 years	Neonates	Neonates	Adults 20-40 years	Adults 20-30 years
Dataset primary purpose	hearing test	hearing test	hearing test	Biometrics	Biometrics

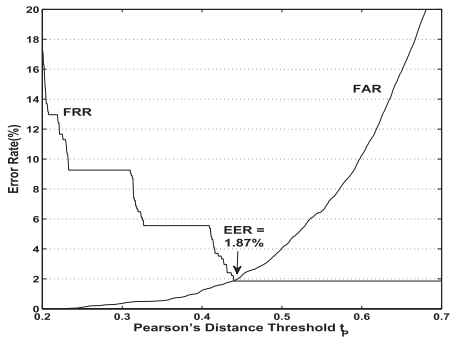

Fig. 8. Verification performance of left ear signal with CWT scale = 8, in close-set scenario.

with previous approaches. Experiments next focus on binaural scenario in order to further improve the system performance by fusing results from both ears. Moreover, performance of proposed method is herein evaluated by cross-validation. It meanwhile evaluates how accurately our proposed system will perform.

B. Single Ear Results

1) Verification Performance: At first, performance of the proposed verification method is measured in false accept rate (FAR), false reject rate (FRR) and EER, i.e., the rate at which FAR and FRR are equal. For example, the performance of left ear signal with CWT scale = 8 is exhibited in Figure 8, which shows a trade-off between FAR and FRR over a broad range of thresholds t_P. An EER 1.87% is obtained when $t_P = 0.440$.

Similarly, Table III displays the EERs under 5 empirical CWT scales without and with subsequent LDA respectively. Results of using previous method proposed in [3] and [15] by approximating PDF upon Euclidean distance of time series data, as well as those of BEMD [2] at 5 most refined levels of intrinsic mode function (IMF) are also appended. Our proposed method obviously outperforms previous ones, with an EER **1.85%** achieved at CWT scale = 7 for the left ear and **0.39%** at CWT scale = 6 for the right. This again proves that analyzing TEOAE signal in only time domain is suboptimal, since its frequency features are neglected. Time-frequency representation based on CWT preserves both time and frequency features of the signal and flexibly extracts a particular component that can best identify itself (e.g., component extracted at scale = 7 for the left ear and 6 for the right). Besides, in open-set scenario, the proposed system also exceeds previous methods, with an EER 9.26% achieved at CWT scale = 8 for the left ear and 6.46% at CWT scale = 9 for the right.

TABLE III
PERFORMANCE IN VERIFICATION (EER) OF THE PROPOSED METHOD UNDER 5 EMPIRICAL CWT SCALES, AND A SIMILAR ONE WITHOUT SUBSEQUENT LDA, AS WELL AS THAT OF PDF ESTIMATE PROPOSED IN [15] AND [3] AND BEMD IN [2]

Method	Property	Left Ear	Right Ear
PDF Estimate	–	38.28 %	36.18 %
BEMD	IMF1	16.77 %	16.63 %
	IMF2	9.72 %	9.26 %
	IMF3	9.33 %	9.26 %
	IMF4	22.19 %	12.96 %
	IMF5	35.22 %	35.53 %
Closed-set (with LDA)	Scale = 6	3.69 %	**0.39 %**
	Scale = 7	**1.85 %**	0.67 %
	Scale = 8	1.87 %	1.85 %
	Scale = 9	3.82 %	1.61 %
	Scale = 10	5.57 %	1.85 %
Open-set (without LDA)	Scale = 6	9.73 %	10.18 %
	Scale = 7	9.27 %	8.33 %
	Scale = 8	**9.26 %**	7.14 %
	Scale = 9	10.39 %	**6.46 %**
	Scale = 10	10.19 %	6.86 %

2) Identifiation Performance: Under the same scheme, the efficiency of the proposed identification approach (CWT+LDA+SR) is compared against that of BEMD followed by matching with the largest pairwise correlation coefficient [2] (Table IV).

The proposed method also exceeds the other classifiers and achieves the best identification rate **94.26%** at scale = 8 for the left ear and **96.30%** at scale = 6 for the right ear. BEMD, on the other hand, successively traces out local oscillation components based on extrema of the original signal. It is highly distorted by noise and not able to efficiently capture a significant trend for differentiation purpose. Besides, LDA effectively reduces the intra-class variability of such physiological signal. For instance, it improves the performance from 92.59% (without LDA) to 94.26% (with LDA) for the left ear at CWT scale = 8.

TABLE IV
PERFORMANCE IN IDENTIFICATION OF THE PROPOSED METHOD UNDER 5 EMPIRICAL CWT SCALES, AND A SIMILAR ONE WITHOUT SUBSEQUENT LDA, AS WELL AS THAT OF BEMD PROPOSED IN [2]

Method	Property	Left Ear	Right Ear
BEMD	IMF1	68.52 %	66.67 %
	IMF2	77.78 %	72.22 %
	IMF3	75.93 %	88.89 %
	IMF4	61.11 %	68.52 %
	IMF5	29.63 %	25.92 %
Without LDA / Proposed	Scale = 6	87.03 % / 90.00 %	92.22 % / **96.30 %**
	Scale = 7	90.00 % / 90.56 %	92.59 % / 95.74 %
	Scale = 8	92.59 % / **94.26 %**	90.74 % / 95.74 %
	Scale = 9	87.03 % / 90.74 %	89.63 % / 95.93 %
	Scale = 10	83.33 % / 85.56 %	88.89 % / 94.44 %

C. Fusion of Both Ears

With promising results from single ear, the goal in fusion scenario is to improve the accuracy and system robustness by integrating information of both ears. Possible fusion strategies for both two modes are discussed as follows:

1) Fusion in Verification: It is implemented based on the distance score computed upon components at CWT scale = 7 for the left ear and score computed at CWT scale = 6 for the right ear. Strategies include:

- *SumScore* - sum up the scores of both ears, i.e., $S_p^{fusion} = S_p^l + S_p^r$.
- *MulScore* - multiply the scores of both ears.
- *MatcherWeighting(MW)Score* [25] - weighted sum of scores of both ears. Weights w^l and w^r are associated with respective EERs eer^l and eer^r achieved in single ear scenario, in the following relation:

$$w^l = \frac{1}{eer^l(1/eer^l + 1/eer^r)}$$
$$w^r = \frac{1}{eer^r(1/eer^l + 1/eer^r)} \quad (15)$$

In order to estimate how efficiently a fusion strategy will function, 2-fold cross-validation is performed, which meanwhile gauges the generalizability of the whole methodology. For each iteration, we shuffle data from the first and second session and split them in two sets d_0 and d_1 which are in equal size. We then train on d_0 and test on d_1 so that training set will not be fixed as data from only one session. Results including EERs and FRRs satisfying zero FAR are finally averaged over 1000 iterations to produce a performance evaluation, which is shown in Table V for close-set scenarios and Table VI for open-set scenarios. Baseline results, i.e., performance in single ear scenario under the same cross-validation scheme, are also included.

With strategy *MWScore*, in close-set protocol, the lowest EER **0.02%** is achieved, and the lowest FRR **1.55%** guaranteeing zero FAR is attained. As for open-set protocol, strategy *MWScore* also yields the best performance, where EER is **3.69%**.

TABLE V
CLOSE-SET VERIFICATION PERFORMANCE OF THE PROPOSED SYSTEM BASED ON DIFFERENT FUSION STRATEGIES

Fusion strategy	EER (mean ± std)	FRR @ 0% FAR (mean ± std)
Left ear only	2.67 % ± 0.93 %	11.96 % ± 4.06 %
Right ear only	0.48 % ± 0.39 %	11.84 % ± 2.31 %
SumScore	0.26 % ± 0.25 %	3.70 % ± 0 %
MulScore	0.12 % ± 0.01 %	2.47 % ± 0.55 %
MWScore	**0.02 % ± 0.02 %**	**1.54 % ± 1.39 %**

TABLE VI
OPEN-SET VERIFICATION PERFORMANCE OF THE PROPOSED SYSTEM BASED ON DIFFERENT FUSION STRATEGIES

Fusion strategy	EER (mean ± std)	FRR @ 0% FAR (mean ± std)
Left ear only	9.02 % ± 0.23 %	31.72 % ± 0.37 %
Right ear only	6.94 % ± 0.45 %	21.75 % ± 0.19 %
SumScore	3.70 % ± 0 %	7.41 % ± 0 %
MulScore	3.71 % ± 0 %	7.41 % ± 0 %
MWScore	**3.69 %** ± 0 %	**7.41 %** ± 0 %

TABLE VII
IDENTIFICATION PERFORMANCE OF THE PROPOSED SYSTEM BASED ON DIFFERENT FUSION STRATEGIES

Fusion strategy	Accuracy (mean ± std)
Left ear only	93.07 % ± 1.33 %
Right ear only	95.45 % ± 0.70 %
MaxScore	97.51 % ± 0.87 %
SumScore	97.62 % ± 0.82 %
MulScore	**99.44 % ± 0.62 %**
SumWtScore	98.23 % ± 1.75 %
SumRank	97.25 % ± 0.95 %
MulRank	98.96 % ± 0.85 %
SumWtRank	98.14 % ± 0.04 %

2) Fusion in Identification: It is operated on the best representation extracted at scale = 8 for the left ear and scale = 7 for the right. Fusion is based on score which is the value of elements in hypothesis vector obtained by Eq. (9), and rank which indicates the descending order of all elements. Possible fusion strategies are as follows:

- *MaxScore* - order by the maximum of the scores, e.g., if the maximum probability of left ear h^l_{max} is larger than that of right ear h^r_{max}, fusion result will be consistent with left ear result.
- *SumScore* - add the scores of both ears, $h^{fusion} = h^l + h^r$.
- *MulScore* - multiply the scores of both ears.
- *SumWtScore* - weighted sum of scores of both ears. Greater weight is assigned to the right ear since it outperforms the left. In this examination, $h^{fusion} = 1 \times h^l + 1.5 \times h^r$.
- *SumRank* - sum up the ranks of both ears.

- *MulRank* - multiply the ranks of both ears.
- *SumWtRank* - similar to *SumWtScore*, $R^{fusion} = 1 \times R^l + 1.5 \times R^r$.

Similarly, Table VII details fusion results averaged over 1000 cross-validation iterations. With strategy MulScore best average accuracy **99.44%** is achieved, as well as the second least variation.

Last but not least, it is worth noting that right ear regularly outperforms left ear. For instance, in verification, individual FAR based on left ear signal is larger than that on right ear signal by a range from -1.88% to 16.79%, and 1.71% in average. This is mainly due to the fact that TEOAE is slightly prominent in the right versus left ear as stated in pervious biological research [26], [27].

VI. Conclusion

In this paper, we have proposed a novel approach to biometric verification based on TEOAE, by resorting to wavelet analysis to derive time-frequency representation of the signal and LDA-based optimal subspace learning algorithm to reduce intra-subject variability. We have presented that the proposed methodology ensures state-of-the-art performance and fusion of information from both ears can further improve accuracy of the biometric system. Future work will focus on extending the scalability to a large population, and multi-biometric system based on TEOAE and other modality/ies.

Acknowledgment

The authors would like to thank Vivosonic Inc. and all participants of the data collection for supporting.

References

[1] T. Matsumoto, H. Matsumoto, K. Yamada, and S. Hoshino, "Impact of artificial 'gummy' fingers on fingerprint systems," *Proc. SPIE*, vol. 4677, pp. 275–289, Jan. 2002.

[2] J. Gao, F. Agrafioti, S. Wang, and D. Hatzinakos, "Transient otoacoustic emissions for biometric recognition," in *Proc. IEEE Int. Conf. Acoust., Speech, Signal Process. (ICASSP)*, Mar. 2012, pp. 2249–2252.

[3] N. J. Grabham *et al.*, "An evaluation of otoacoustic emissions as a biometric," *IEEE Trans. Inf. Forensics Security*, vol. 8, no. 1, pp. 174–183, Jan. 2013.

[4] Y. Liu and D. Hatzinakos, "Biometric identification based on transient evoked otoacoustic emission," in *Proc. IEEE Int. Symp. Signal Process. Inf. Technol.*, Dec. 2013, pp. 267–271.

[5] R. Probst, B. L. Lonsbury-Martin, and G. K. Martin, "A review of otoacoustic emissions," *J. Acoust. Soc. Amer.*, vol. 89, no. 5, pp. 2027–2067, 1991.

[6] J. Hall, *Handbook of Otoacoustic Emissions* (A Singular Audiology Text). San Diego, CA, USA: Singular Publ. Group, 2000.

[7] M. S. Robinette and T. J. Glattke, *Otoacoustic Emissions: Clinical Applications*, 3rd ed. New York, NY, USA: Thieme, 2007.

[8] G. Zimatore, A. Giuliani, S. Hatzopoulos, A. Martini, and A. Colosimo, "Invariant and subject-dependent features of otoacoustic emissions," in *Proc. 3rd Int. Symp. Med. Data Anal.*, 2002, pp. 158–166.

[9] J. W. Hall, J. E. Baer, P. A. Chase, and M. K. Schwaber, "Sex differences in distortion-product and transient-evoked otoacoustic emissions compared," *J. Acoust. Soc. Amer.*, vol. 125, no. 1, pp. 239–246, 2009.

[10] *Transient Otoacoustic Emissions (TEOAE)*. Biometrics Security Lab. Univ. Toronto. [Online]. Available: http://www.comm.utoronto.ca/~biometrics/databases

[11] H. P. Wit, J. C. Langevoort, and R. J. Ritsma, "Frequency spectra of cochlear acoustic emissions ('Kemp-echoes')," *J. Acoust. Soc. Amer.*, vol. 70, no. 2, pp. 437–445, 1981.

[12] A. Grzanka, W. Konopka, S. Hatzopoulos, and P. Zalewski, "TEOAE high resolution time-frequency components and their long term stability," in *Proc. 17th Biennial Symp. Int. Evoked Response Audiometry Study Group (IERASG)*, 2001, p. 36.

[13] W. Konopka, A. Grzanka, and P. Zalewski, "Personal long-term reproducibility of the TEOAE time-frequency distributions," *Polish J. Otolaryngol.*, vol. 56, no. 6, pp. 701–706, 2002.

[14] M. A. Swabey, S. P. Beeby, A. D. Brown, and J. E. Chad, "Using otoacoustic emissions as a biometric," in *Proc. Int. Conf. Biometric Authentication (ICBA)*, 2004, pp. 600–606.

[15] M. A. Swabey *et al.*, "The biometric potential of transient otoacoustic emissions," *Int. J. Biometrics*, vol. 1, no. 3, pp. 349–364, Mar. 2009.

[16] P. Chambers, N. J. Grabham, and M. A. Swabey, "A comparison of verification in the temporal and cepstrum-transformed domains of transient evoked otoacoustic emissions for biometric identification," *Int. J. Biometrics*, vol. 3, no. 3, pp. 246–264, 2011.

[17] G. Tognola, F. Grandori, and P. Ravazzani, "Wavelet analysis of click-evoked otoacoustic emissions," *IEEE Trans. Biomed. Eng.*, vol. 45, no. 6, pp. 686–697, Jun. 1998.

[18] F. Hlawatsch and G. F. Boudreaux-bartels, "Linear and quadratic time-frequency signal representations," *IEEE Signal Process. Mag.*, vol. 9, no. 2, pp. 21–67, Apr. 1992.

[19] I. Daubechies, *Ten Lectures on Wavelets*. Philadelphia, PA, USA: SIAM, 1992.

[20] P. Belhumeur, J. P. Hespanha, and D. J. Kriegman, "Eigenfaces vs. fisherfaces: Recognition using class specific linear projection," *IEEE Trans. Pattern Anal. Mach. Intell.*, vol. 19, no. 7, pp. 711–720, Jul. 1997.

[21] B.-H. Juang and S. Katagiri, "Discriminative learning for minimum error classification [pattern recognition]," *IEEE Trans. Signal Process.*, vol. 40, no. 12, pp. 3043–3054, Dec. 1992.

[22] D. Böhning, "Multinomial logistic regression algorithm," *Ann. Inst. Statist. Math.*, vol. 44, no. 1, pp. 197–200, 1992.

[23] B. Krishnapuram, L. Carin, M. A. T. Figueiredo, and A. J. Hartemink, "Sparse multinomial logistic regression: Fast algorithms and generalization bounds," *IEEE Trans. Pattern Anal. Mach. Intell.*, vol. 27, no. 6, pp. 957–968, Jun. 2005.

[24] D. C. Liu and J. Nocedal, "On the limited memory BFGS method for large scale optimization," *Math. Program.*, vol. 45, no. 3, pp. 503–528, Dec. 1989. [Online]. Available: http://dx.doi.org/10.1007/BF01589116

[25] R. Snelick, U. Uludag, A. Mink, M. Indovina, and A. Jain, "Large-scale evaluation of multimodal biometric authentication using state-of-the-art systems," *IEEE Trans. Pattern Anal. Mach. Intell.*, vol. 27, no. 3, pp. 450–455, Mar. 2005.

[26] M. S. Robinette, "Clinical observations with transient evoked otoacoustic emissions with adults," *Seminars Hearing*, vol. 13, no. 1, pp. 23–26, 1992.

[27] J. W. Hall, J. E. Baer, P. A. Chase, and M. K. Schwaber, "Clinical application of otoacoustic emissions: What do we know about factors influencing measurement and analysis?" *Otolaryngol. Head Neck Surgery*, vol. 110, no. 1, pp. 22–38, 1994.

Yuxi Liu received the B.Sc. degree from Sun Yat-sen University, Guangzhou, China, in 2012. He is currently pursuing the M.A.Sc. degree with the Edward S. Rogers Sr. Department of Electrical and Computer Engineering, University of Toronto, Toronto, ON, Canada. His research interests include biometric systems, multimedia signal processing, and machine learning and pattern recognition. He is a member of the Biometrics Security Laboratory with the University of Toronto.

Dimitrios Hatzinakos (M'90–SM'98) received the Diploma degree from the University of Thessaloniki, Thessaloniki, Greece, in 1983, the M.A.Sc. degree from the University of Ottawa, ON, Canada, in 1986, and the Ph.D. degree from Northeastern University, Boston, MA, USA, in 1990, all in electrical engineering. In September 1990, he joined the Department of Electrical and Computer Engineering, University of Toronto, Toronto, ON, Canada, where he currently holds the rank of Tenure Professor. He served as the Chair of the Communications Group with the Department of Electrical and Computer Engineering from 1999 to 2004. Since 2004, he has held the Bell Canada Chair in Multimedia with the University of Toronto. He is also the Director and Chair of the Management Committee with the Identity, Privacy and Security Institute, University of Toronto. His research interests are in the areas of multimedia signal processsing, multimedia security, multimedia communications, and biometric systems. He has authored or coauthored over 230 papers in technical journals and conference proceedings, and contributed to 14 books in his areas of interest. His experience includes consulting through Electrical Engineering Consociates Ltd., Toronto, and contracts with United Signals and Systems, Inc., Culver City, CA, USA, Burns and Fry Ltd., Toronto, Pipetronix Ltd., Toronto, Defense Research and Development Canada, Ottawa, Nortel Networks, Mississauga, ON, Canada, Vivosonic Inc, Etobicoke, ON, Canada, CANAMET Inc., North York, ON, Canada, and Ontario Lottery and Gaming Corporation, Toronto. He is currently an Associate Editor of the IEEE TRANSACTIONS ON MOBILE COMPUTING. He has served as an Associate Editor of the IEEE TRANSACTIONS ON SIGNAL PROCESSING from 1998 to 2002, and a Guest Editor of the special issue *Signal Processing* (Elsevier) on Signal Processing Technologies for Short Burst Wireless Communications in 2000. He was a member of the IEEE Statistical Signal and Array Processing Technical Committee from 1992 to 1995, and the Technical Program Cochair of the 5th Workshop on Higher-Order Statistics in 1997. He is a member of the European Association for Signal Processing, the Professional Engineers of Ontario, and the Technical Chamber of Greece.